



## Fenofibrate enhances barrier function of endothelial continuum within the metastatic niche of prostate cancer cells

Katarzyna Piwowarczyk, Ewa Wybieralska, Jarosław Baran, Julia Borowczyk, Paulina Rybak, Milena Kosińska, Anna Julia Włodarczyk, Marta Michalik, Maciej Siedlar, Zbigniew Madeja, Jerzy Dobrucki, Krzysztof Reiss & Jarosław Czyż

To cite this article: Katarzyna Piwowarczyk, Ewa Wybieralska, Jarosław Baran, Julia Borowczyk, Paulina Rybak, Milena Kosińska, Anna Julia Włodarczyk, Marta Michalik, Maciej Siedlar, Zbigniew Madeja, Jerzy Dobrucki, Krzysztof Reiss & Jarosław Czyż (2015) Fenofibrate enhances barrier function of endothelial continuum within the metastatic niche of prostate cancer cells, *Expert Opinion on Therapeutic Targets*, 19:2, 163-176, DOI: [10.1517/14728222.2014.981153](https://doi.org/10.1517/14728222.2014.981153)

To link to this article: <https://doi.org/10.1517/14728222.2014.981153>

 View supplementary material [↗](#)

 Published online: 12 Nov 2014.

 Submit your article to this journal [↗](#)

 Article views: 1820

 View related articles [↗](#)

 View Crossmark data [↗](#)

 Citing articles: 6 View citing articles [↗](#)

# EXPERT OPINION

1. Introduction
2. Methods
3. Results
4. Discussion
5. Conclusions

**informa**  
healthcare

## Fenofibrate enhances barrier function of endothelial continuum within the metastatic niche of prostate cancer cells

Katarzyna Piwowarczyk, Ewa Wybieralska, Jarosław Baran, Julia Borowczyk, Paulina Rybak, Milena Kosińska, Anna Julia Włodarczyk, Marta Michalik, Maciej Siedlar, Zbigniew Madeja, Jerzy Dobrucki, Krzysztof Reiss & Jarosław Czyż<sup>†</sup>

<sup>†</sup>Jagiellonian University, Department of Cell Biology, Faculty of Biochemistry, Biophysics and Biotechnology, Krakow, Poland

**Objective:** Extravasation of circulating cancer cells is an important step of the metastatic cascade and a potential target for anti-cancer strategies based on vasoprotective drugs. Reports on anti-cancer effects of fenofibrate (FF) prompted us to analyze its influence on the endothelial barrier function during prostate cancer cell diapedesis.

**Research design and methods:** *In vitro* co-cultures of endothelial cells with cancer cells imitate the 'metastatic niche' *in vivo*. We qualitatively and quantitatively estimated the effect of 25  $\mu$ M FF on the events which accompany prostate carcinoma cell diapedesis, with the special emphasis on endothelial cell mobilization.

**Results:** Fenofibrate attenuated cancer cell diapedesis via augmenting endothelial cell adhesion to the substratum rather than through the effect on intercellular communication networks within the metastatic niche. The inhibition of endothelial cell motility was accompanied by the activation of PPAR $\alpha$ -dependent and PPAR $\alpha$ -independent reactive oxygen species signaling, Akt and focal adhesion kinase (FAK) phosphorylation, in the absence of cytotoxic effects in endothelial cells.

**Conclusions:** Fenofibrate reduces endothelial cell susceptibility to the paracrine signals received from prostate carcinoma cells, thus inhibiting endothelial cell mobilization and reducing paracellular permeability of endothelium in the metastatic niche. Our data provide a mechanistic rationale for extending the clinical use of FF and for the combination of this well tolerated vasoactive drug with the existing multidrug regimens used in prostate cancer therapy.

**Keywords:** endothelium, fenofibrate, invasion, PPAR $\alpha$ , prostate cancer, reactive oxygen species

*Expert Opin. Ther. Targets* (2015) 19(2):163-176

### 1. Introduction

Agonists of PPARs are known to control the expression of genes involved in glucose and lipid metabolism. They have been used in the treatment of diabetes, hyperlipidemia and cardiovascular diseases [1,2]. Fenofibrate (propan-2-yl 2-[4-[(4-chlorophenyl) carbonyl] phenoxy]-2-methylpropanoate) is an FDA-approved, PPAR $\alpha$  agonist characterized by excellent safety and tolerability profile after chronic and prolonged treatments [3,4]. It is widely used in clinical practice to lower serum levels of triglycerides and cholesterol, improve low-density lipoproteins; high-density lipoproteins ratio and prevent atherosclerosis [5-8]. In parallel, the vascular protecting

activity of fenofibrate (FF), independent of its lipid-lowering activity, has been reported, including its activity in improving physiological neovascularization [9-11]. Conversely, several reports indicate that FF may suppress endothelial cell proliferation and migration, leading to the attenuation of tumor vasculature [12-15]. Vascularization of primary tumors and the interactions of cancer cells with endothelial continua are crucial for cancer development [16,17]; therefore, these facts prompted questions about possible application of FF in cancer therapy [18].

According to the simplified model of cancer promotion and progression, the formation of extensively proliferating cell subpopulations characterizes early steps of carcinogenesis, while cancer progression is triggered by the clonal appearance of cells, capable of invading distant organs [19]. Potential interference of FF with cancer promotion was illustrated by the attenuation of growth and survival of glioblastoma [20], hepatoma [21,22], medulloblastoma [23] and melanoma cells [24]. At the level of cancer progression, FF was demonstrated to reduce invasive potential of cancer cells [24-27]. Both these activities have been ascribed to PPAR $\alpha$  activation [3,24,26,28-30] but also to the PPAR $\alpha$ -independent effect of FF on the accumulation of reactive oxygen species (ROS) [21,31]. Importantly, ROS have been implicated in the PPAR $\alpha$ -dependent [26] and PPAR $\alpha$ -independent [27] inhibition of cancer cell motility. Converging effects of FF on endothelial and cancer cell properties, its excellent safety and tolerability profile along with anti-inflammatory activity [32], warrant the intensive investigations into the possible interference of FF with the progression of cancers characterized by long latency periods, such as prostate cancer.

Penetration of the endothelial layer lining up vessel walls by circulating cancer cells (cancer cell diapedesis) is a multistep process, which determines the effectiveness of the metastatic cascade and malignant dissemination [33]. It is initiated by the stabilization of cancer cell adhesion to the endothelial layer inside microcapillaries [34-36] and followed by local remodeling of endothelial continuum in the 'metastatic niche' of cancer cells. Prompted by previous reports on the interference of FF with tumor vasculature [15], we undertook an in-depth examination of its effects on endothelial reactivity to the signals generated by cancer cells. Monitoring of the events accompanying the penetration of endothelial continuum by DU-145 cells gave us the opportunity to recapitulate the complexity of systems that regulate endothelial susceptibility to challenge by a single cancer cell. This approach enabled us to comprehensively address FF effects on the efficiency of prostate carcinoma cell diapedesis.

## 2. Methods

### 2.1 Cell culture

Human umbilical vein endothelial cells (HUVECs, Life Technologies Corp.) were routinely cultured in endothelial basal medium (EBM) supplemented with 10% fetal bovine serum (FBS) and supplement cocktail (recombinant human

epidermal growth factor [rhEGF], bovine brain extract, hydrocortisone, gentamicin, amphotericin-B; all from Lonza). For end point experiments, the cells were used within 2-6 passages in serum-free EBM medium with supplements. Human prostate carcinoma DU-145 and PC-3 cells were routinely cultivated in DMEM-F12 HAM (Sigma) medium supplemented with 10% FBS and antibiotics [37]. Co-culture experiments were performed on HUVEC monolayers between 70 and 98% confluence (indicated in the text). DU-145 or PC-3 cells were seeded into HUVEC cultures at the density of 1300 cells/cm<sup>2</sup> in serum-free conditions. Fenofibrate, GW9662 and N-acetyl-L-cysteine (NAC; all from Sigma) were administered at the time points and concentration(s) indicated in the text.

### 2.2 Immunocytochemistry and fluorescence microscopy

For the immunofluorescence analysis, cells on coverslips were fixed with 3.7% formaldehyde (20 min), permeabilized (0.1% Triton X-100 in PBS, 5 min), blocked with 3% BSA and incubated with a primary antibody (rabbit polyclonal anti-VE-cadherin IgG, mouse monoclonal anti-vinculin IgG, mouse monoclonal anti-ZO-1 IgG; all from Sigma; [38]). Subsequently, the cells were stained with a secondary antibody (Alexa Fluor 488-conjugated goat anti-rabbit IgG or Alexa Fluor 488-conjugated goat anti-mouse IgG; Life Technologies), and counterstained with TRITC-conjugated phalloidin and/or Hoechst 33258 (both from Sigma). Where indicated, cancer cells were stained with CellTracker Orange CMRA (10  $\mu$ M, Invitrogen). For gap junctional intercellular coupling (GJIC) analyses, calcein-loaded (Invitrogen) donor (DU-145) cells were plated on monolayers of acceptor (HUVEC) cells grown on coverslips in Petri dishes at the ratio of 1:50 [39] to evaluate intercellular calcein transfer and coupling index defined as the percentage of donor cells coupled with at least one acceptor cell. To determine the cytotoxic effect of FF, HUVECs incubated with various concentrations of FF for 6, 24 and 48 h were harvested, and the number of viable cells was determined by the fluorescence diacetate/ethidium bromide test. Image acquisition was performed with a Leica DMI6000B microscope (DMI7000 version; Leica Microsystems, Wetzlar, Germany) equipped with the Total Internal Reflection Fluorescence, Nomarski Differential Interference Contrast (DIC) and Interference Modulation Contrast (IMC) modules. LAS-AF deconvolution software was used for image processing as described previously [39]. Three dimensional (3D) images were registered using a Leica TCS SP5 confocal microscope (Leica Microsystems, Mannheim, Germany) using 63 $\times$  HCX PL APO CS oil immersion (NA 1.4) objective lens. The following instrumental parameters were used: excitation 405 nm (pulsed), 488 nm (Ar) and 543 nm (HeNe); emission detection bands: 430 nm - 480 nm for Hoechst (DNA counterstaining), and 500 nm - 575 nm for AlexaFluor488 or 560 nm - 630 nm (for TRITC);

voxel size:  $70 \times 70 \times 210$  nm, registration in sequential mode, scanning 700 Hz,  $4 \times$  line-averaged. 3D stacks of images were deconvolved and visualized as 3D projections using SVI 3D Huygens Deconvolution & Analysis Software (Scientific Volume Imaging B.V., Hilversum, Netherlands).

### 2.3 Transmigration and transendothelial permeability assays

HUVECs were seeded on coverslips at  $2 \times 10^4$  cells/well and grown to confluence for 72 h. Thereafter, 1300 DU-145 or PC-3 cells/cm<sup>2</sup> were seeded on a HUVEC monolayer on coverslips and incubated for 6 and 24 h, before F-actin/DNA staining and microscopic estimation of the percentage of cancer cells capable of disrupting the endothelial continuum (endothelial penetration index-EPI). For permeability studies, HUVECs were plated at  $1 \times 10^5$  cells into polycarbonate Transwell inserts (3  $\mu$ m pore size, 6.5 mm diameter; Corning) and nonadherent cells were removed after 6 h. Inserts were used for experiments 3 days after plating and transendothelial permeability was measured as previously described [40]. Briefly, fluorescein isothiocyanate (FITC)-dextran (MW 42000; 1 mg/ml) was added to the upper compartment of Transwell after 6 h of FF and/or DU-145 cell addition in serum-free media. Samples were taken after 15 min, 30 min and 1 h from the lower compartment and equal volume of media was re-added to the lower chamber. The amount of FITC-dextran was determined with a microplate reader Infinite M200PRO (Tecan Group Ltd.), using excitation wavelength of 492 nm and emission detection at 521 nm. All inserts were fixed and then stained with eozine and phenol red after the experiment to verify the confluence and general appearance of the HUVEC monolayer.

### 2.4 Cell motility

The movement of HUVECs in mono- and co-cultures was time-lapse recorded using Leica DMI6000B time-lapse system equipped with a temperature chamber ( $37 \pm 0.2^\circ\text{C}/5\% \text{CO}_2$ ), IMC contrast optics and a cooled, digital DFC360FX CCD camera. HUVECs were seeded at density of 500 cells/cm<sup>2</sup> and cultured for 4 days to form islets (70% confluence). Then cultures were treated with FF and/or GW9662/NAC and recorded for 7 h with 5 min intervals. In the case of co-culture, 1300 DU-145 or PC-3 cells/cm<sup>2</sup> were added to endothelial cell culture, recorded for 7 h and only HUVECs that had direct contact with cancer cells were analyzed. The tracks of individual cells were determined from a series of changes in the cell centroid positions. The data were pooled and analyzed to estimate basic cell motility parameters, including: i) total length of the cell trajectory ( $\mu$ m); ii) the total length of cell displacement, that is, the distance from the starting point directly to the cell's final position ( $\mu$ m); iii) the average speed of cell movement, that is, total length of cell trajectory/time of recording ( $\mu$ m/h); and iv) the average rate of cell displacement, that is, the distance from the starting

point directly to the cell's final position/time of recording ( $\mu$ m/h). Cell trajectories from no less than three independent experiments (number of cells > 50) were obtained for analysis by the non-parametric Mann-Whitney test [41].

### 2.5 FACS analyses of ROS

HUVECs in mono- and co-cultures with DU-145 cells were treated with the EGM medium containing 25  $\mu$ M FF and/or 10  $\mu$ M GW9662/5 mM NAC, in the presence of DHR 123 (dihydrorhodamine 123; 2  $\mu$ M, Life Technologies) for 4 h. Subsequently, the cells were harvested, washed and suspended in PBS. Measurements of DHR 123 fluorescence intensity were carried out with a FACSCalibur flow cytometer (Becton Dickinson; excitation - 488 nm).

### 2.6 Immunoblotting and angiogenic protein arrays

Cells for immunoblotting were dissolved in a lysis buffer, cellular proteins (20  $\mu$ g/lane) were applied to 10% SDS-polyacrylamide gels, followed by transfer to a nitrocellulose membrane. Membranes were exposed to primary antibody (rabbit monoclonal anti-pSer473Akt IgG, rabbit monoclonal anti-Akt IgG, rabbit polyclonal anti-pThr202/pTyr204 Erk1/2 IgG, rabbit anti-Erk1/2 IgG, rabbit monoclonal anti-pTyrFAK IgG, rabbit monoclonal anti-Focal Adhesion Kinase [FAK] IgG (all from Cell Signalling); mouse monoclonal anti-vinculin IgG, mouse anti- $\alpha$ -tubulin IgG and mouse anti-actin IgG (all from Sigma)) followed by counterstaining with relevant HRP-conjugated secondary antibody (Invitrogen), their detection and semiquantification with SuperSignal West Pico Substrate (Pierce, Rockford, IL) and the MicroChemii imaging system (SNR Bio-Imaging Systems, Jerusalem, Israel) [42]. Angiogenesis-related protein expression in HUVECs was estimated by semiquantitative technique based on antibody array kit (Proteome Profiler™ Human Angiogenesis Array Kit, R&D Systems) according to the manufacturer's protocol. Samples were mixed with a cocktail of biotinylated detection antibodies and then incubated with nitrocellulose membranes to enable their binding to cognate immobilized capture antibodies, detection with streptavidin-HRP and semiquantification with the MicroChemii imaging system and Quantity One software. The signal was produced at each spot in proportion to the amount of the analyte bound. The results were expressed as fold changes above or below the relevant control.

### 2.7 Quantitative reverse transcription polymerase chain reaction

Total mRNA from the cells was prepared using the RNeasy Mini Kit Plus (Qiagen, Inc.) and reverse-transcribed with high capacity reverse transcription kit (Applied Biosystems). Detection of vinculin and glyceraldehyde 3-phosphate dehydrogenase (GAPDH) levels was performed by real-time reverse transcription polymerase chain reaction (RT-PCR) assay using 7500Fast System (Applied Biosystems). For detection of specific cDNAs, TaqMan gene expression assay was

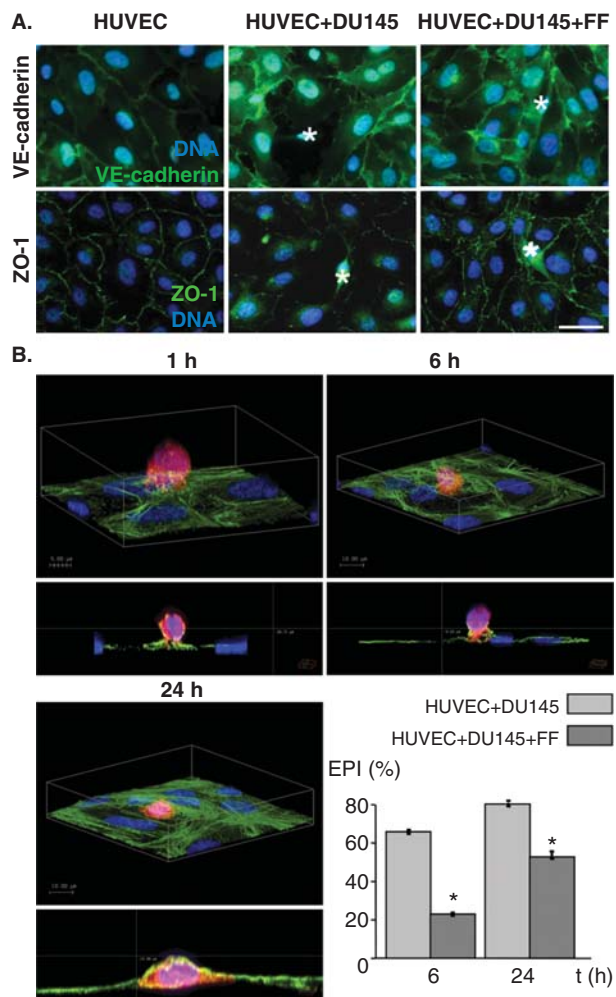


**Figure 1. Fenofibrate inhibits penetration of endothelial layers by DU-145 cells.** **A.** DU-145 cells (marked with \*) were seeded onto the monolayer of HUVECs (98% confluence, serum-free; left) at the density of 1300 cells/cm<sup>2</sup> in the absence (middle) or presence of 25  $\mu$ M FF (right). After 6 h, specimens were fixed with 3.7% FA, permeabilized, stained for VE-cadherin (upper panel) or ZO-1 (lower panel) and counterstained with Hoechst33258. **B.** Representative XY and XZ reconstructions of transmigrating DU-145 cells registered 1, 6 and 24 h. after seeding in the absence of FF. DU-145 cells were stained with CellTracker, seeded and fixed as in **A**, stained against F-actin, counterstained with Hoechst33258 and visualized with confocal laser scanning microscopy. Transendothelial penetration indices were estimated for DU-145 cells seeded onto the HUVEC monolayer in the absence and presence of FF at the indicated time points. Statistical significance versus the relevant control at  $p < 0.01$  (t-Student test,  $n = 3$ ). Scale bar - 40  $\mu$ m. Note that attenuating effect of FF on a disruption of intercellular contacts within the endothelium in the proximity of DU-145 correlates with delayed penetration of DU-145 through endothelial layers in the presence of 25  $\mu$ M FF. All results are representative of three independent experiments.

FA: Focal adhesion; HUVECs: Human umbilical vein endothelial cells.

used including 6-carboxyfluorescein-labeled probes: Hs00419715 m1 (vinculin) and Hs99999905\_m1 (GAPDH) (Applied Biosystems). GAPDH was used as a reference gene. Results are presented as a  $\Delta\Delta$ Ct value.

## 2.8 Statistical analysis

The statistical significance was determined by the Student's t-test with  $p < 0.01$  (transmigration, fluorimetric and viability tests) or  $p < 0.05$  (qRT-PCR) considered to indicate significant differences; by the non-parametric Mann-Whitney test ( $p < 0.01$ ; time-lapse analyses) and Wilcoxon signed-rank test ( $p < 0.05$ ; permeability tests). Each parameter was calculated as the mean and standard error of the mean.

## 3. Results

### 3.1 Fenofibrate enhances endothelial barrier function to DU-145 cells

We used co-cultures of HUVECs with human prostate carcinoma DU-145 cells to estimate the effect of FF on the efficiency of DU-145 cell diapedesis. Confluent monolayers of adherent HUVECs imitate the endothelial layer at the interface between the blood and the interstitial tissues. VE-cadherin-mediated intercellular adhesion, together with ZO-1-dependent tight junctions, stabilized endothelial integrity *in vitro* (Figure 1A). Disturbance of adherents and tight junctions was observed in the proximity of DU-145 cells shortly after their seeding onto confluent endothelial cells in control conditions. Concomitantly, DU-145 cells efficiently penetrated endothelial layer as visualized and quantified by confocal microscopy (Figure 1B). The value of EPI estimated in control conditions increased from 66 to 79% between 6th and 24th hour of co-incubation. 25  $\mu$ M FF considerably delayed transendothelial penetration of DU-145 cells (EPI = 24 and 55% after 6 and 24 h of co-incubation, respectively). This effect was accompanied by less prominent disturbances of endothelial continuum in the presence of FF (Figure 1A).

### 3.2 Fenofibrate targets DU-145-induced HUVEC mobilization

Actin cytoskeleton determines endothelial barrier function through the effect on endothelial cell adhesion [43]. Therefore, we further estimated the effect of DU-145 cells on actin cytoskeleton organisation in HUVEC. Short and scattered stress fibers attached to relatively small focal adhesions (FAs), were accompanied by cortical belts of F-actin in control HUVECs in serum-free conditions (Figure 2A). The seeding of DU-145 cells evoked reorganization of F-actin in proximal HUVECs, which was illustrated by the formation of prominent stress fibers and FAs. Concomitant time-lapse analyses of proximal HUVECs revealed an induction of their motility in subconfluent co-cultures with DU-145 cells (Figure 2B). These data demonstrate that cancer cells affect endothelial barrier function through the mobilization of endothelial cells.

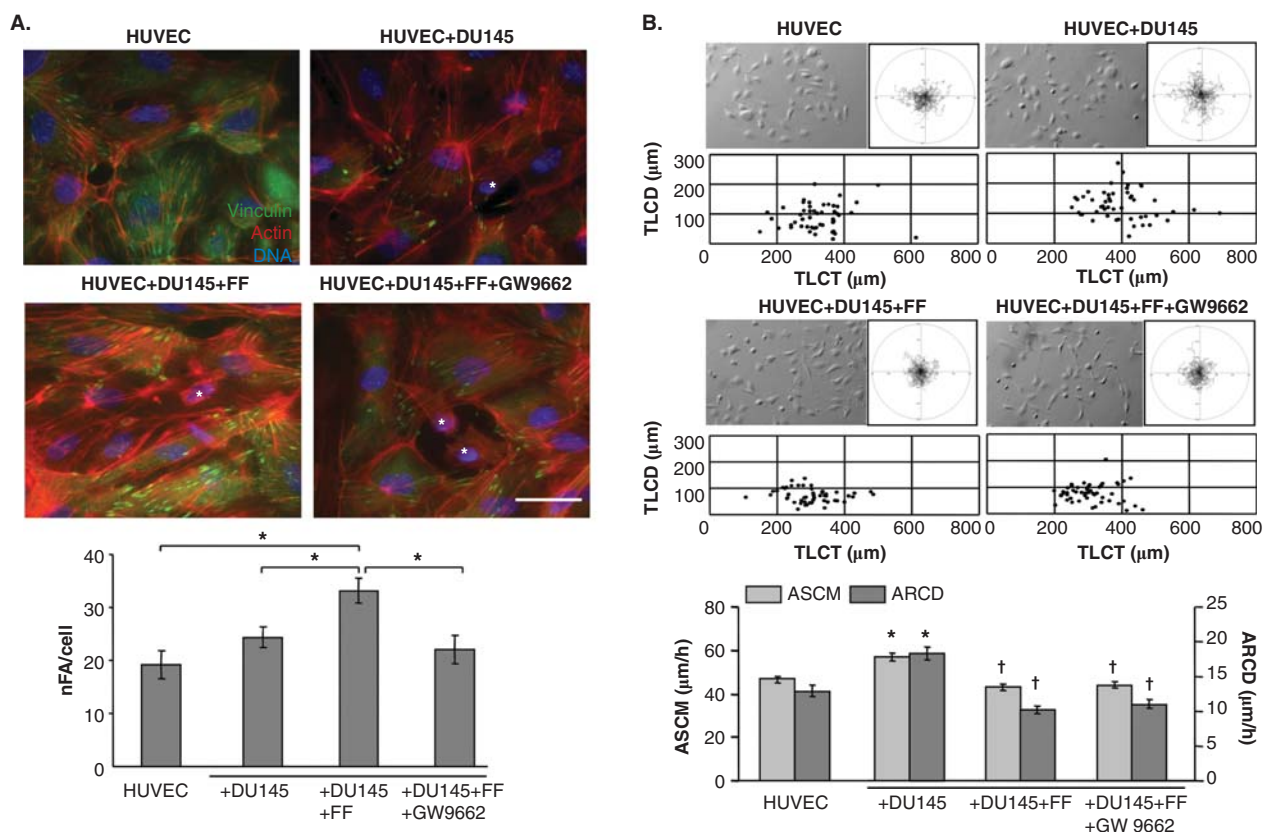


**Figure 2. Fenofibrate evokes cytoskeletal rearrangements and reduces DU-145-induced HUVEC motility.** **A.** DU-145 cells (marked with \*) were seeded onto the monolayer of HUVECs at the density of 1300 cells/cm<sup>2</sup> in the absence (upper right), in the presence of 25 μM FF (lower left), or in the presence of 25 μM FF and 10 μM GW9662 (lower right). After 24 h, specimens were fixed with 3.7% FA, permeabilized, and stained for F-actin and vinculin. A number of FAs per single cell was calculated and plotted from TIRF photomicrographs. Statistical significance versus the relevant control at *p* < 0.01 (Student's *t*-test, *n* = 3). **B.** HUVEC motility was visualized by time-lapse videomicroscopy in the conditions ascertaining their basal motility (70% confluence). Cells were analyzed in the control (serum-free) conditions (upper left), in the presence of DU-145 cells (upper right), in the presence of DU-145 cells and 25 μM FF (lower left), or in the presence of DU-145 cells, 25 μM FF and 10 μM GW9662 (lower right). Cell trajectories are depicted as circular diagrams (axis scale in μm) drawn with the initial point of each trajectory placed at the origin of the plot (registered for 7 h; *n* > 50). Inserts depict cell morphology visualized by IMC. Dot-plots and column chart show movement parameters of proximal cells at the single cell and population level, respectively. Statistical significance was estimated with the non-parametric Mann-Whitney test. Error bars represent SEM. Scale bar: 25 μm. Note that increased sizes and numbers of vinculin<sup>(+)</sup> FAs in FF-treated HUVECs correlate with their attenuated motility. GW9662 counteracts the effects of FF on HUVEC cytoskeleton but not on their motility. All results are representative of three independent experiments.

\* vs HUVEC control; † vs HUVEC+DU-145; *p* ≤ 0.01

FAs: Focal adhesions; HUVECs: Human umbilical vein endothelial cells; IMC: Interference Modulation Contrast; siRNA: Small interfering RNA; SEM: Standard error of the mean; TIRF: Total internal reflection fluorescence.

Noteworthy, the enhancement of endothelial barrier function by FF (Figure 1) was correlated with its inhibitory effect on DU-145-induced HUVEC motility (Figure 2B). In contrast, a synergy of FF and DU-145 effects on HUVEC cytoskeleton was illustrated by increased numbers of mature FAs and more prominent stress fibers in proximal HUVECs cultivated in the presence of FF (Figure 2A). Corresponding effects of FF on HUVEC mobilization by human prostate cancer PC-3 were observed (Figure S1 in supplementary data). Thus, augmentation of HUVEC adhesion to underlying extracellular matrix

may reduce their susceptibility to the signals from cancer cells and improve endothelial barrier function.

Because FF was found to exert its biological effects through the activation of PPARα/ROS-dependent signaling [3], we further estimated how PPAR antagonist GW9662 influenced the effect of FF on HUVEC mobilization by DU-145 cells. GW9662 attenuated FF-induced cytoskeleton reorganization (Figure 2A) but failed to restore FF-inhibited HUVEC motility in the co-cultures with DU-145 cells (Figure 2B). Similar correlation was observed in HUVEC/PC-3 co-cultures

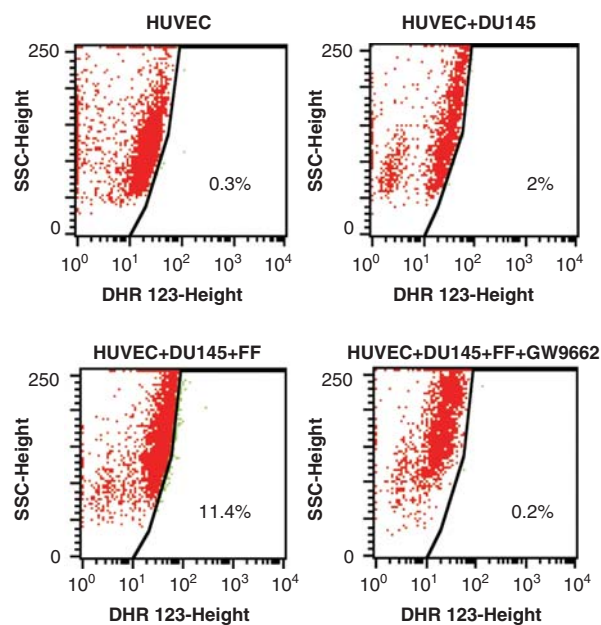


**Figure 3. Fenofibrate induces ROS production in HUVECs co-cultured with DU-145 cells in a PPAR $\alpha$  – dependent manner.** DU-145 cells were seeded onto the monolayer (98% of confluence; serum-free) of HUVECs at the density of 1300 cells/cm<sup>2</sup> in the absence (upper right), in the presence of 25  $\mu$ M FF (lower left), or in the presence of 25  $\mu$ M FF and 10  $\mu$ M GW9662 (lower right). Co-cultures were incubated in the presence of DHR123 (2  $\mu$ M) for 4 h and analyzed with FACSCalibur flow cytometer. DHR123-specific signal was collected in green channel (505 nm – 560 nm). Dot-plots comprise 20,000 events gated according to SSD properties. Inserts show data quantification according to the gates indicated in the plots. All results are representative of three independent experiments.

HUVECs: Human umbilical vein endothelial cells; ROS: Reactive oxygen species.

(Figure S1 in supplementary data). These effects were accompanied by ROS generation in FF-treated HUVEC/DU-145 co-cultures and downregulation of ROS levels by GW9662 (Figure 3). Because 10  $\mu$ M GW9662 inhibits the activity of PPAR $\alpha$  [44], our data indicate that FF attenuates DU-145-induced HUVEC mobilization at least partly through PPAR $\alpha$ /ROS-dependent effect on the adhesive status of HUVECs. However, PPAR $\alpha$ -independent pathways may also be involved in HUVEC reactions to FF.

### 3.3 Fenofibrate improves endothelial barrier function independently of intercellular communication in the ‘metastatic niche’

FF may directly target endothelial cells or enhance their barrier function through indirect effect on the efficiency of intercellular communication loops in the metastatic niche. Paracrine loops and GJIC between cancer and endothelial cells has long been suggested to facilitate cancer cell diapedesis [33,45]. Actually, FF significantly reduced GJIC intensity

between DU-145 cells and HUVECs. However, this effect was not counteracted by GW9662 (Figure 4A). Furthermore, transient silencing of Cx43 expression in DU-145 cells attenuated their mobilizing effect on HUVEC motility but chemical block of GJIC by 18- $\alpha$ -glycyrrhetic acid exerted only minute effects on HUVEC motility and transendothelial penetration of DU-145 cells (Figure 4B). Thus, interference of FF with GJIC is hardly responsible for its effect on HUVEC mobilization in co-cultures, nor could the augmentation of endothelial barrier function by FF be ascribed to its interference with paracrine loops in the metastatic niche. The shifts in the expression profiles of 22 out of 55 analyzed angioactive factors were seen after DU-145 cell seeding on HUVEC monolayers. Only CXCL16 expression was considerably upregulated in HUVEC/DU-145 co-cultures, whereas downregulation of anti-angiogenic endostatin and of pro-angiogenic IGFBP-2, angiopoietin-2, uPA and TGF- $\beta$ 1 was seen. FF attenuated the expression of pro-angiogenic IGFBP-1 and IL-8, and of anti-angiogenic TIMP-4, TIMP-1, but had no effect on the CXCL16 expression levels in co-cultures (Figure 4C, Figure S2 in supplementary data).

Mobilization of HUVECs and the shifts in the expression of angioactive factors were accompanied by increased extracellular signal-regulated kinase (ERK)1/2-dependent (ERK)1/2-dependent signaling activity in HUVECs co-cultured with DU-145 cells (Figure 4D, see also Figure 2). A pronounced and prolonged ERK1/2 and Akt phosphorylation was seen when FBS depletion was followed by DU145 cell seeding. FF slightly increased ERK1/2 phosphorylation in co-cultures but did not considerably affect ERK1/2 phosphorylation in HUVEC monolayers. In contrast, we observed increased levels of phosphorylated Akt both in FF-treated HUVEC monolayers and HUVEC/DU-145 cultures. Interestingly, the dynamics of Akt phosphorylation in HUVECs upon DU-145 seeding was more similar to control. These data indirectly indicate the involvement of Akt -dependent pathway in the augmentation of endothelial barrier function by FF.

### 3.4 Fenofibrate enhances endothelial barrier function through the direct effect on endothelial cell adhesion

Further analyses of HUVEC reactions to FF administered in the absence of DU-145 cells unequivocally confirmed its direct effect on endothelial cells. Akt phosphorylation (Figure 4) was accompanied by oscillations of FAK phosphorylation levels and correlated with up-regulation of vinculin levels in HUVECs at the protein but not mRNA level (Figure 5A). In conjunction with cytoskeletal rearrangements, in particular with the increased numbers of FAs in FF-treated HUVECs (Figure 5B), this observation is indicative of the recruitment and sequestration of vinculin to FAs. In similar to co-cultures, FF induced cytoskeletal rearrangements and accumulation of ROS in HUVECs (Figure 5C) in a

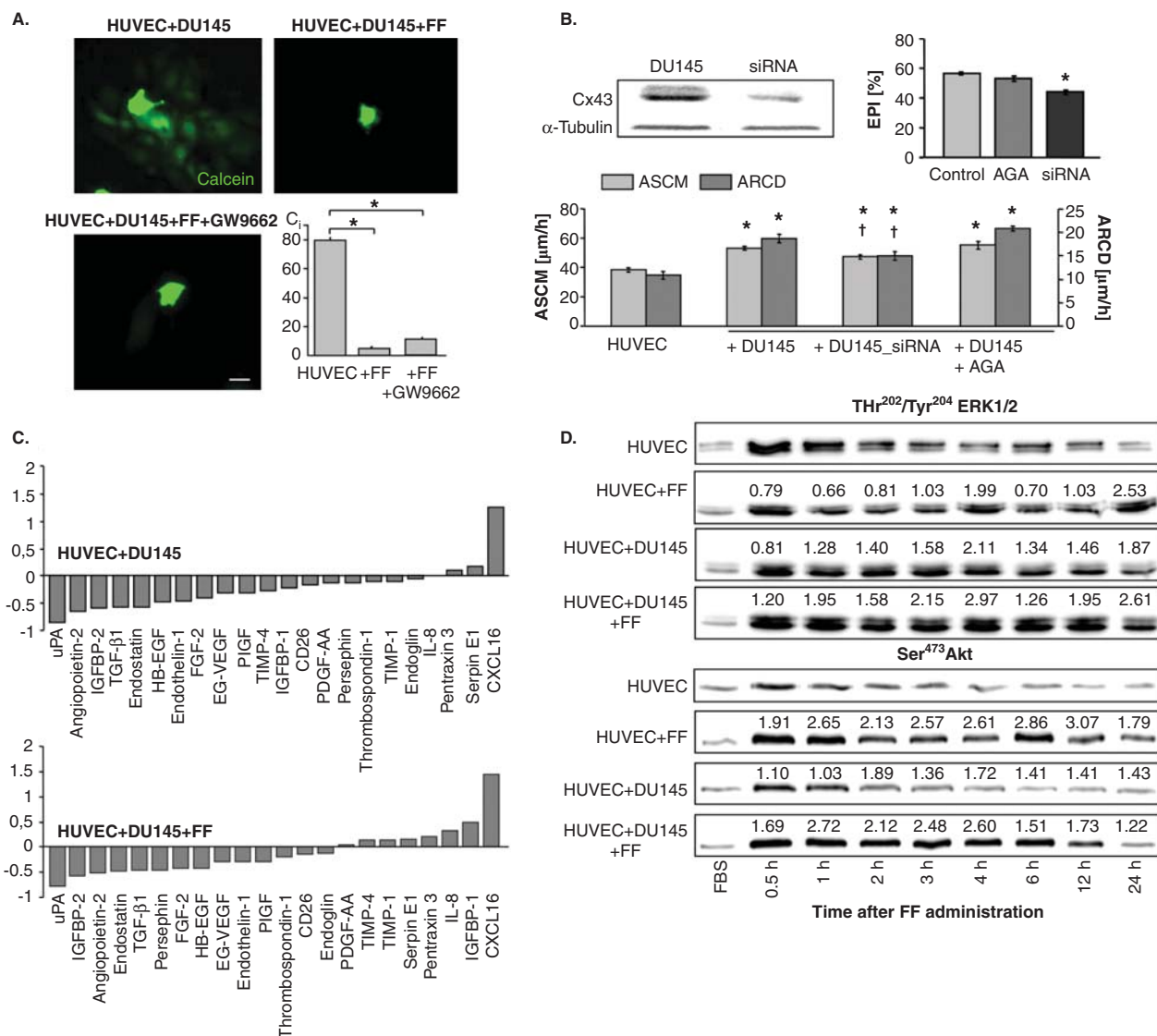


**Figure 4. Communication networks within the metastatic niche do not participate in augmentation of HUVEC barrier function by fenofibrate.** **A.** Calcein-loaded DU-145 cells were seeded onto HUVEC monolayers (98% of confluence) in the absence (upper left), in the presence of 25  $\mu$ M FF (upper right) or in the presence of FF and GW9662 (lower left). The inhibitory effect of FF on GJIC in HUVEC/DU-145 co-cultures is illustrated by quantification of calcein transfer assay (coupling index,  $C_i$ , lower right; 2 h). Statistical significance versus the relevant control at  $p < 0.01$  (t-Student test,  $n = 3$ ). Scale bar: 25  $\mu$ m. **B.** The effect of siRNA Cx43 silencing in DU-145 cells and AGA (100  $\mu$ M) on EPI and HUVEC motility was compared (see legend to Figure 1 and 2). Statistical significance was estimated with the non-parametric Mann-Whitney test (\* vs HUVEC control; † vs HUVEC+DU-145;  $p \leq 0.01$ ). Error bars represent SEM. **C.** HUVECs were cultured in control conditions (98% of confluence), in the presence of DU-145 cells, and in the presence of DU-145 cells and 25  $\mu$ M FF for 24 h. Then, expression of angiogenic proteins was estimated by semiquantitative technique based on antibody array kit (see Methods). Plots show the densitometrically estimated dot intensities illustrating the protein amounts in HUVEC/DU-145 co-cultures in the absence and in the presence of 25  $\mu$ M FF relative to HUVEC control. Note that FF had minute effect on the expression pattern of angiogenic factors in the co-cultures. **D.** HUVEC/DU-145 co-cultures were established as in C, and pSer473Akt and pThr202/pTyr204 ERK1/2 levels were visualized by immunoblotting at the indicated time points in the absence and presence of 25  $\mu$ M FF. Numerical values represent results of densitometric analyses, normalized against housekeeping gene expression ( $\alpha$ -tubulin) and FBS control and compared to control (HUVEC = 1). Note the increase of ERK1/2 and Akt phosphorylation in HUVECs in co-cultures with DU-145, and of Akt phosphorylation in the presence of 25  $\mu$ M FF, respectively. Results are representative of three independent experiments.

AGA: 18- $\alpha$ -glycyrrhetic acid; EPI: Endothelial Penetration Index; FBS: Foetal bovine serum; GJIC: Gap junctional intercellular coupling; HUVECs: Human umbilical vein endothelial cells; SEM: Standard error of the mean.

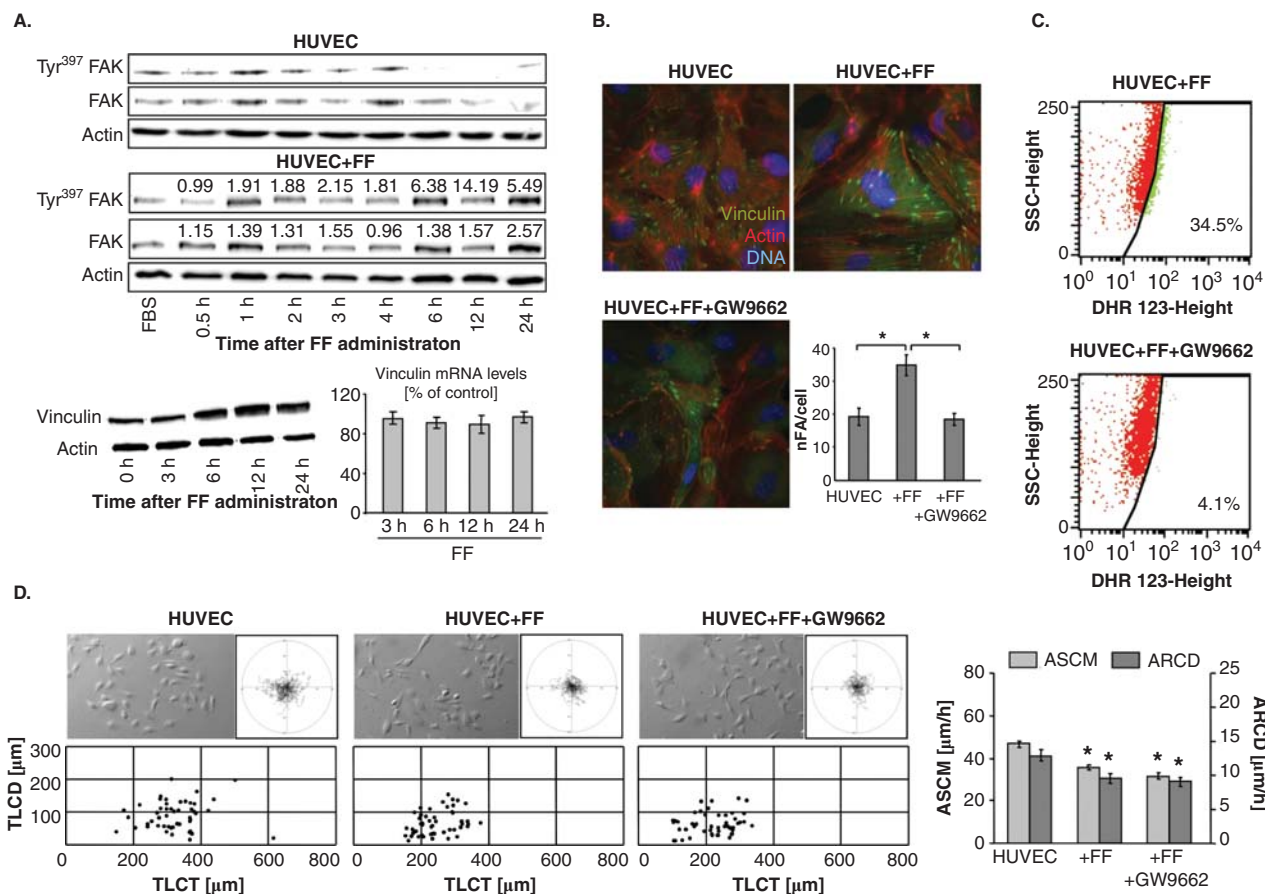


**Figure 5. Fenofibrate directly targets endothelial cell cytoskeleton and motility.** **A.** HUVECs were cultivated in the absence or in the presence of 25  $\mu\text{M}$  FF. Tyr397FAK levels and vinculin expression at protein and mRNA level were analyzed at the indicated time points by immunoblotting and qRT-PCR (quantified as described in Figure 4D). **B.** Cytoskeletal architecture of HUVECs cultured in control conditions (upper left), in the presence of 25  $\mu\text{M}$  FF (upper right), or in the presence of 25  $\mu\text{M}$  FF + 10  $\mu\text{M}$  GW9662 (lower left) was visualized and the numbers of FAs per single cell quantified as in Figure 2 (lower right). **C.** HUVECs (98% of confluence) were cultivated in the presence of 25  $\mu\text{M}$  FF (upper plot), or in the presence of 25  $\mu\text{M}$  FF and 10  $\mu\text{M}$  GW9662 (lower plot). Cells were incubated in the presence of DHR123 (2  $\mu\text{M}$ ) for 4 h and analyzed with FACSCalibur flow cytometer as in Figure 3. **D.** HUVEC motility in the control conditions (70% of confluence; left), in the presence of 25  $\mu\text{M}$  FF (middle left) 25  $\mu\text{M}$  FF + 10  $\mu\text{M}$  GW9662 (middle right) was visualized by time-lapse videomicroscopy and analyzed as in Figure 2B (right). Statistical significance was estimated with the non-parametric Mann-Whitney test (\* vs HUVEC control;  $p \leq 0.01$ ). Error bars represent SEM. Results are representative of three independent experiments.

FAs: Focal adhesions; HUVECs: Human umbilical vein endothelial cells; SEM: Standard error of the mean.

PPAR $\alpha$ -dependent manner because both reactions were attenuated by GW9662 (Figure 5C cf. B). Notably, GW9662 did not counteract inhibitory effect of FF on HUVEC motility (Figure 5D). These findings confirm that FF directly enhances endothelial barrier function partly via direct PPAR $\alpha$ -dependent effects on endothelial cell adhesion.

On the other hand, the lack of GW9662 effects on FF-treated HUVEC motility suggested the involvement of PPAR-independent pathways in HUVEC reactions to FF. Because we observed intracellular ROS accumulation in HUVECs after FF treatment, PPAR $\alpha$ -independent/ROS-dependent pathways may be involved in the observed phenomena. To verify this notion, we analyzed the effect of

NAC on HUVEC reactions to FF. NAC attenuated FF-induced cytoskeletal rearrangements (Figure 6A) and significantly restored FF-inhibited HUVEC motility (Figure 6B). NAC strengthens cellular antioxidant defense systems [46], therefore these findings would confirm an involvement of PPAR $\alpha$ -independent/ROS-dependent signaling in the determination of HUVEC responses to FF. On the other hand, eradication of HUVEC responses to FF by NAC was accompanied by the increase of ROS levels in FF-treated cells (Figure 6C). Notably, FF did not influence the structure of tight junctions in HUVEC monolayers and its effect on their permeability to solutes was similar in the presence and absence of DU-145 cells (Figure 7A). No

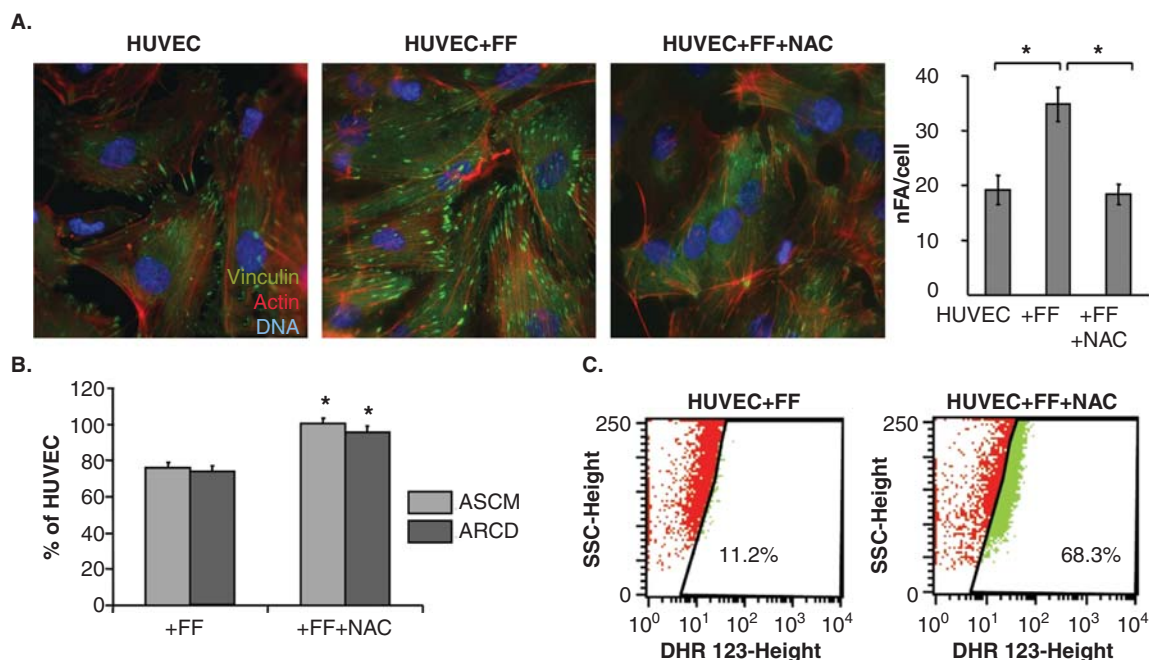


**Figure 6. PPAR $\alpha$ -independent signaling is involved in the augmentation of endothelial barrier function by fenofibrate.** **A.** Cytoskeletal architecture of HUVECs cultured in control conditions (left), in the presence of 25  $\mu$ M FF (middle left), 25  $\mu$ M FF + 5 mM NAC (middle right) is visualized and the numbers of FAs per single cell quantified as in Figure 2 (right). Statistical significance versus the relevant control at  $p < 0.01$  (t-Student test,  $n = 3$ ). **B.** HUVEC motility in the control conditions (70% of confluence), in the presence of 25  $\mu$ M FF and 25  $\mu$ M FF + 5 mM NAC was visualized by time-lapse videomicroscopy and analyzed as in Figure 2B. Statistical significance versus the relevant control at  $p < 0.01$  (t-Student test,  $n = 3$ ). **C.** HUVEC monolayers (98% of confluence) treated with 25  $\mu$ M FF (left), or with 25  $\mu$ M FF and 5 mM NAC (right) were incubated in the presence of DHR123 and analyzed with FACSCalibur flow-cytometer as in Figure 3. Note that NAC abrogates HUVEC reactions to FF but does not down-regulate intracellular ROS levels.

FAs: Focal adhesions; HUVECs: Human umbilical vein endothelial cells; NAC: N-acetyl-L-cysteine; ROS: Reactive oxygen species.

pronounced changes in the expression pattern of angioactive factors were seen either (Figure 7B). When administered at concentrations of up to 100  $\mu$ M, FF prompted the maturation of focal contacts and reduced their motility in a dose-dependent fashion, but exerted no effects on their viability (Figure 7C; Table 1). NAC-induced normalization of HUVEC phenotype in the presence of high ROS levels indicates the involvement of a discrete ROS pool in HUVEC-reactions to FF. Thus, ROS generation is a physiological response of endothelial cells to FF, unrelated to FF cytotoxicity.

#### 4. Discussion

Penetration of endothelial layer by circulating cancer cells is a prerequisite for their homing in interstitial compartments underlying the endothelium. This process is crucial for the metastatic cascade [47] and its efficiency depends on a number of intrinsic cancer cell traits: their motile activity and nano-mechanical elasticity, competence for GJIC, expression of cell adhesion receptors and secretion of metalloproteinases [34,48-50]. The interference of FF with tumor progression has predominantly been considered in terms of its effect on these

properties [23,26]. The susceptibility of the endothelial layer to a challenge by a single cancer cell is an equally important, yet underestimated determinant of diapedesis [48,51]. FF effect on the properties of endothelial continuum in the metastatic niche has not yet been assessed. This study fills this gap because it demonstrates for the first time that FF enhances endothelial barrier function through the direct effect on endothelial cell susceptibility to the signals generated by prostate cancer cells. The influence of FF on endothelial cell behavior in the metastatic niche illustrates a new mechanism of its anti-cancer activity. It confirms previous suggestions about the interference of FF with the metastatic cascade which were based on *in vivo* approaches [18,25]. It is noteworthy that the enhancement of endothelial barrier function to prostate cancer cells was observed in the presence of 25  $\mu$ M FF. This concentration of FF in the culture medium remains within the limits defined by the content of fenofibric acid, an active FF metabolite, in the blood of patients who take FF on regular bases (up to 200 mg/day). Pharmacodynamic studies have revealed that maximal concentrations of fenofibric acid in the sera of FF-treated patients considerably exceed 25  $\mu$ M [52-55], confirming the biological significance of our findings.

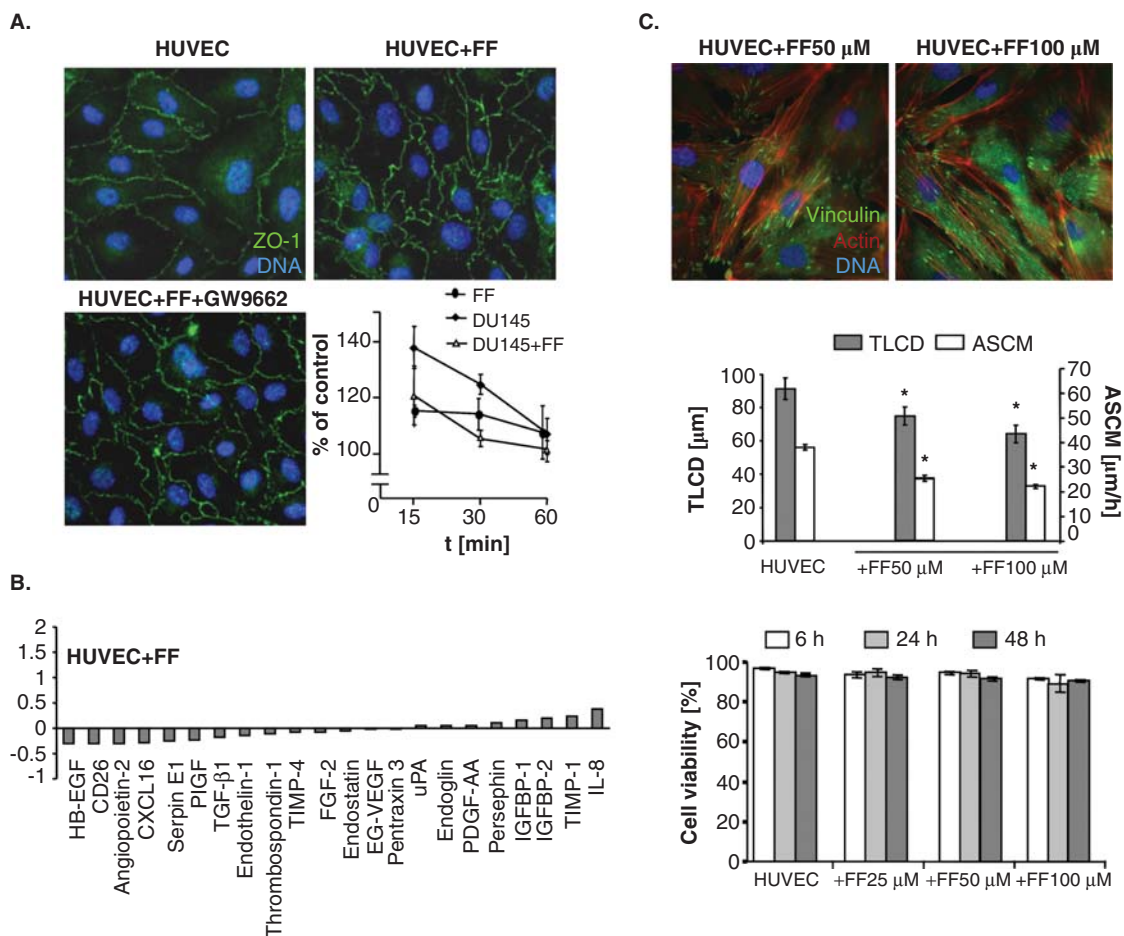


**Figure 7. FF does not exert sub-lethal effects in HUVECs.** **A.** Functional status of ZO-1-mediated intercellular contacts in control conditions (upper left), in the presence of 25  $\mu$ M FF (upper right), or in the presence of 25  $\mu$ M FF + 10  $\mu$ M GW9662 (lower left); and the effect of DU-145 and 25  $\mu$ M FF on solute permeability of HUVEC monolayers was analyzed as described (see Figure 1 and Methods, respectively). **B.** HUVECs were cultured in control conditions (98% of confluence) and in the presence of 25  $\mu$ M FF for 24 h. Then, angiogenic proteins were analyzed as in Figure 4B. **C.** HUVECs were cultivated in the presence of FF (25-100  $\mu$ M) and their cytoskeleton architecture (see Figure 6A for control; upper panel) motility (middle), and viability (lower plot) was quantified. Statistical significance: \* versus the relevant control at  $p < 0.01$ , using the Wilcoxon signed-rank test (A), Mann-Whitney (B) and Student t-test (C). Note the dose-dependent effects of FF on HUVEC cytoskeleton and motility but not on HUVEC viability.

HUVECs: Human umbilical vein endothelial cells.

**Table 1. Effect of fenofibrate on the motile activity of HUVECs.**

Parameters	Control	FF 25 $\mu$ M	FF 50 $\mu$ M	FF 100 $\mu$ M
TLCT ( $\mu$ m)	391.8 $\pm$ 11.5	308.5 $\pm$ 14.7*	271.4 $\pm$ 11.3*	229.8 $\pm$ 9.1*
ASCM ( $\mu$ m/h)	55.9 $\pm$ 1.6	44.1 $\pm$ 2.1*	38.8 $\pm$ 1.6*	32.8 $\pm$ 1.3*
TLCD ( $\mu$ m)	91.1 $\pm$ 6.5	82.9 $\pm$ 7.5	77.6 $\pm$ 5.6*	63.9 $\pm$ 5.3*
ARCD ( $\mu$ m/h)	13.0 $\pm$ 0.9	11.8 $\pm$ 1.1	11.1 $\pm$ 0.8*	9.1 $\pm$ 0.7*

Values are the means  $\pm$  SEM.

\*Statistically significant (Mann-Whitney test) at  $p \leq 0.01$  (HUVEC in control conditions vs HUVEC treated with fenofibrate at indicated concentrations).

ARCD: Average rate of cell displacement; ASCM: Average speed of cell movement; HUVECs: Human umbilical vein endothelial cells; SEM: Standard error of the mean; TLCD: Total length of cell displacement; TLCT: Total length of cell trajectory.

Monitoring of endothelial cell behavior in the proximity of cancer cells gives the opportunity to reconstruct the events in the 'metastatic niche' of circulating cancer cells during cancer cell diapedesis. It provides a tool to evaluate the role of endothelial cell mobilization in the progress of the transendothelial penetration of cancer cells. DU-145 cell line, which was used in this study to imitate circulating prostate carcinoma cells, had been propagated from prostate cancer metastases to brain. Thus, DU-145 cells represent the progeny of cells capable of penetrating tissue barriers. The interference of FF with their intrinsic properties might thus have participated in the observed attenuation of transendothelial penetration in HUVEC/DU-145 co-cultures. Actually, we have previously shown that FF inhibits the motility and GJIC in DU-145 populations [27]. Here, we observed the retraction of endothelium in the proximity of DU-145 cells, which was accompanied by induction of HUVEC motility and counteracted by FF. Interference of FF with endothelial cell mobilization by PC-3 cells (derived from prostate cancer metastasis to bone) additionally illustrates the biological significance of our data. Corresponding HUVEC responses to FF seen in the absence and presence of cancer cells show that FF effectors are situated down-stream of intercellular communication loops within the metastatic niche. FF inhibited GJIC between cancer and endothelial cells [56], but this communication route plays a secondary role in HUVEC mobilization by DU-145 cells. Concomitantly, the expression of angioactive factors, which might mobilize HUVECs in the ERK1/2-dependent manner, was not affected by FF. These data indicate that FF enhances endothelial barrier function in the 'metastatic niche' of prostate cancer cells through a direct effect on endothelial cell properties.

PPAR $\alpha$ /ROS-dependent pathway has previously been implicated in the inhibition of cancer cell invasive potential [26]. Our observations indicate that PPAR $\alpha$ -dependent, ROS-dependent signaling is also involved in the regulation of endothelial barrier function in the 'metastatic niche' by FF. This was illustrated by a partial abrogation of endothelial cell responses to FF seen in the presence of PPAR $\alpha$  antagonist. It was accompanied by attenuation of ROS accumulation in FF-treated HUVECs. Akt and FAK phosphorylation observed in FF-treated HUVECs suggest that both effectors participate in the endothelial cell reactions to FF. Notably, it has previously been shown that endothelial cell reactions (incl. inhibition of cell motility and angiogenesis) to FF and other PPAR $\alpha$  agonists are mediated by Akt [57]. Whether Akt provides a mechanistic link between PPAR $\alpha$  pathway and cytoskeletal rearrangements in endothelial cells requires a more elaborate study based on PPAR $\alpha$  knock-out approach. Such an approach should also consider the interrelations between FF-induced ROS signaling in HUVEC and activation of Akt-dependent pathway.

More detailed analyses are also required to identify mechanisms underlying the abrogation of FF effect on endothelial cells by NAC. Concomitantly with the attenuation of FF-induced cytoskeletal rearrangements, NAC restored the

motility of FF-treated HUVECs. It demonstrates the involvement of PPAR $\alpha$ -independent, ROS-dependent pathway in HUVEC reactions to FF. Such a pathway has been shown to mediate FF-induced inhibition of cell motility [27]. As a glutathione (GSH) precursor, NAC assists intracellular antioxidant defense systems [46]. However, it failed to reduce ROS levels in FF-treated endothelial cells. In the absence of FF effects on endothelial cell viability, these observations suggest the involvement of a discrete, relatively small ROS partition, generated in a PPAR $\alpha$ -independent fashion. Preventive effect of NAC on GSH depletion in FF-treated endothelial cells, which reduces their susceptibility to ROS signaling, may provide an alternative explanation for this conundrum. Precise identification of the specific, NAC-sensitive and NAC-insensitive ROS and their subcellular origin(s) is needed to justify further speculations on the mechanisms of ROS involvement in endothelial cell reactions to FF *in vitro* and *in vivo*.

Considering the present state of knowledge, we can again only speculate about the mechanisms of the interplay between PPAR $\alpha$ -dependent/independent pathways and adhesion of FF-treated HUVECs [12,57]. Stress fibers thickening, increased vinculin expression and FA recruitment [58] in FF-treated endothelial cells are characteristic for strongly adherent isometrically contracting cells [59]. We can suggest that FAK-dependent adhesive status of endothelial cells cooperates in the regulation of endothelial barrier function. Increased solute permeability of FF-treated endothelia suggests that the shifts in cell adhesion strength may evoke changes in the equilibrium between cell-to-cell and cell-substratum interactions, crucial for endothelial barrier function [33]. However, local loosening of intra-endothelial fascia adherens can only be sufficient for transendothelial infiltration of 'ameboid' cells, such as leukocytes or monocytes. These cells are elastic enough to squeeze through relatively small endothelial discontinuities [60]. In contrast, cancer cells that are characterized by 'mesenchymal' strategy of movement display relatively low susceptibility to mechanical distortions [61]. They require more prominent endothelial remodeling to penetrate trans-junctional windows. Whereas DU-145 cell motility plays a secondary role in the remodeling of endothelial continuum, the inhibition of endothelial cell motility may additionally strengthen endothelial barrier function through stabilizing effect on cell-substratum adhesion. Negative feedback loops between cell migration and adhesion strength may participate in this process. Thus, converging FF effects on cancer and endothelial cells at the 'metastatic niche' affect the susceptibility of the endothelial continuum to the signals from cancer cells and regulate endothelial barrier function.

## 5. Conclusions

The *in vitro* model, which imitates the interface between circulating cancer cells and endothelium [34,48,62], enabled us to demonstrate the attenuating effect of FF on endothelial cell

responsiveness to the signals generated by cancer cells in the metastatic niche. The strengthening effect of FF on endothelial cell adhesion and impairment of motile activity by FF reduces the efficiency of prostate carcinoma cell diapedesis and potentially interferes with the prostate cancer metastatic cascade. In the context of other *in vivo* studies that directly and/or indirectly suggest the interference of FF with tumor progression [15,18,25], this report extends the knowledge on biological effects of existing and emerging vasoactive drugs on the metastatic cascade. It fills the gap in the understanding of the links between the vasoactive, anti-atherosclerotic and anti-tumorigenic activity of FF and suggests the application of this lipid-lowering drug as a means to reducing the metastatic spread of prostate cancer cells. It also justifies further analyses of the interference of FF with the metastatic cascade of prostate cancer and other tumors with the more sophisticated genetic *in vivo* approaches. Comprehensive epidemiologic studies are also postulated to estimate the links between FF intake and risk of prostate cancer metastases.

## Bibliography

Papers of special note have been highlighted as either of interest (●) or of considerable interest (●●) to readers.

- Lamers C, Schubert-Zsilavecz M, Merk D. Therapeutic modulators of peroxisome proliferator-activated receptors (PPAR): a patent review (2008-present). *Expert Opin Ther Pat* 2012;22:803-41
- Ahmed W, Ziouzenkova O, Brown J, et al. PPARs and their metabolic modulation: new mechanisms for transcriptional regulation? *J Intern Med* 2007;262:184-98
- Grabacka M, Reiss K. Anticancer properties of PPARalpha-effects on cellular metabolism and inflammation. *PPAR Res* 2008;2008:930705
- Grabacka M, Pierzchalska M, Reiss K. Peroxisome proliferator activated receptor alpha ligands as anticancer drugs targeting mitochondrial metabolism. *Curr Pharm Biotechnol* 2013;14:342-56
- Robinson JG. LDL reduction: how low should we go and is it safe? *Curr Cardiol Rep* 2008;10:481-7
- Adeghate E, Adem A, Hasan MY, et al. Medicinal chemistry and actions of dual and Pan PPAR modulators. *Open Med Chem J* 2011;5:93-8

- Balakumar P, Rohilla A, Mahadevan N. Pleiotropic actions of fenofibrate on the heart. *Pharmacol Res* 2011;63:8-12
- This paper critically discusses pleiotropic actions of fenofibrate (FF) on the heart beyond its lipid-lowering effects, in particular vascular endothelial dysfunction-associated cardiovascular abnormalities.**
- McKeage K, Keating GM. Fenofibrate: a review of its use in dyslipidaemia. *Drugs* 2011;71:1917-46
- Katayama A, Yamamoto Y, Tanaka K, et al. Fenofibrate enhances neovascularization in a murine ischemic hindlimb model. *J Cardiovasc Pharmacol* 2009;54:399-404
- Hiukka A, Maranghi M, Matikainen N, et al. PPARalpha: an emerging therapeutic target in diabetic microvascular damage. *Nat Rev Endocrinol* 2010;6:454-63
- Noonan JE, Jenkins AJ, Ma JX, et al. An update on the molecular actions of fenofibrate and its clinical effects on diabetic retinopathy and other microvascular end points in patients with diabetes. *Diabetes* 2013;62:3968-75
- Goetze S, Eilers F, Bungenstock A, et al. PPAR activators inhibit endothelial cell migration by targeting Akt. *Biochem Biophys Res Commun* 2002;293:1431-7

- Varet J, Vincent L, Mirshahi P, et al. Fenofibrate inhibits angiogenesis *in vitro* and *in vivo*. *Cell Mol Life Sci* 2003;60:810-19
- One of the first studies to directly show inhibitory effect of FF on endothelial cell proliferation, migration and capillary tube formation *in vitro*, and angiogenesis *in vivo*.**
- Meissner M, Stein M, Urbich C, et al. PPARalpha activators inhibit vascular endothelial growth factor receptor-2 expression by repressing Sp1-dependent DNA binding and transactivation. *Circ Res* 2004;94:324-32
- Panigrahy D, Kaipainen A, Huang S, et al. PPARalpha agonist fenofibrate suppresses tumor growth through direct and indirect angiogenesis inhibition. *Proc Natl Acad Sci USA* 2008;105:985-90
- This study shows that PPARalpha activation by ligands cause tumor suppression by the inhibition of angiogenesis. It has formulated mechanistic rationale for evaluating the clinical benefits of fenofibrate in the treatment of progressed cancers.**
- Cao Z, Shang B, Zhang G, et al. Tumor cell-mediated neovascularization and lymphangiogenesis contrive tumor progression and cancer metastasis. *Biochim Biophys Acta* 2013;1836:273-86
- This review comprehensively discusses the significance of neovasculogenesis**

## Declaration of interest

This work was financially supported by the Polish National Science Centre (grant 2011/01/B/NZ3/00004) and funds granted to the Faculty of Biochemistry, Biophysics and Biotechnology of Jagiellonian University to further “The Development of Young Scientists and Doctoral Students” 2011/2012 (DS/46/2011). The Faculty of Biochemistry, Biophysics and Biotechnology of the Jagiellonian University is a beneficiary of the structural funds from the European Union (Grants No: UDA-POIG.01.03.01-14-036/09-00 - “Application of polyisoprenoid derivatives as drug carriers and metabolism regulators”; POIG.02.01.00-12-064/08 - “Molecular biotechnology for health”; POIG 01.02-00-109/99 “Innovative methods of stem cell applications in medicine”). The authors declare that they have no competing interests. The authors have no other relevant affiliations or financial involvement with any organization or entity with a financial interest in or financial conflict with the subject matter or materials discussed in the manuscript apart from those disclosed.

- for cancer progression and the role of paracrine loops between cancer and endothelial cells in this process.**
17. Hida K, Ohga N, Akiyama K, et al. Heterogeneity of tumor endothelial cells. *Cancer Sci* 2013;104:1391-5
  - **The significance of heterogeneity in tumor endothelial cells for cancer development and therapy is discussed in this mini-review.**
  18. Robison NJ, Campigotto F, Chi SN, et al. A phase II trial of a multi-agent oral antiangiogenic (metronomic) regimen in children with recurrent or progressive cancer. *Pediatr Blood Cancer* 2014;61:636-42
  - **A study that shows application of fenofibrate in a potentially efficient '5-drug' oral regimen in children with recurrent or progressive cancer.**
  19. Langley RR, Fidler IJ. The seed and soil hypothesis revisited—the role of tumor-stroma interactions in metastasis to different organs. *Int J Cancer* 2011;128:2527-35
  20. Giordano A, Macaluso M. Fenofibrate triggers apoptosis of glioblastoma cells in vitro: new insights for therapy. *Cell Cycle* 2012;11:3154
  21. Jiao HL, Zhao BL. Cytotoxic effect of peroxisome proliferator fenofibrate on human HepG2 hepatoma cell line and relevant mechanisms. *Toxicol Appl Pharmacol* 2002;185:172-9
  22. Yamasaki D, Kawabe N, Nakamura H, et al. Fenofibrate suppresses growth of the human hepatocellular carcinoma cell via PPARalpha-independent mechanisms. *Eur J Cell Biol* 2011;90:657-64
  23. Urbanska K, Pannizzo P, Grabacka M, et al. Activation of PPARalpha inhibits IGF-I-mediated growth and survival responses in medulloblastoma cell lines. *Int J Cancer* 2008;123:1015-24
  24. Grabacka M, Plonka PM, Urbanska K, et al. Peroxisome proliferator-activated receptor alpha activation decreases metastatic potential of melanoma cells in vitro via down-regulation of Akt. *Clin Cancer Res* 2006;12:3028-36
  25. Grabacka M, Placha W, Plonka PM, et al. Inhibition of melanoma metastases by fenofibrate. *Arch Dermatol Res* 2004;296:54-8
  - **To our knowledge, the first study to demonstrate anti-metastatic activity of fenofibrate in vivo.**
  26. Drukala J, Urbanska K, Wilk A, et al. ROS accumulation and IGF-IR inhibition contribute to fenofibrate/PPARalpha-mediated inhibition of Glioma cell motility in vitro. *Mol Cancer* 2010;9:159
  27. Wybierska E, Szpak K, Gorecki A, et al. Fenofibrate attenuates contact-stimulated cell motility and gap junctional coupling in DU-145 human prostate cancer cell populations. *Oncol Rep* 2011;26:447-53
  28. Thuillier P, Anchiraico GJ, Nickel KP, et al. Activators of peroxisome proliferator-activated receptor-alpha partially inhibit mouse skin tumor promotion. *Mol Carcinog* 2000;29:134-42
  29. Saidi SA, Holland CM, Charnock-Jones DS, et al. In vitro and in vivo effects of the PPAR-alpha agonists fenofibrate and retinoic acid in endometrial cancer. *Mol Cancer* 2006;5:13
  30. Panigrahy D, Kaipainen A, Kieran MW, et al. PPARs: a double-edged sword in cancer therapy? *PPAR Res* 2008;2008:350351
  31. Scatena R, Bottoni P, Giardina B. Mitochondria, PPARs, and cancer: is receptor-independent action of PPAR agonists a key? *PPAR Res* 2008;2008:256251
  - **This review summarizes extrareceptor activities of synthetic PPAR ligands and their consequences for the application of PPAR activators in clinics.**
  32. Tomizawa A, Hattori Y, Inoue T, et al. Fenofibrate suppresses microvascular inflammation and apoptosis through adenosine monophosphate-activated protein kinase activation. *Metabolism* 2011;60:513-22
  - **The study demonstrating that fenofibrate might exert a protective effect on the microvasculature through AMP-activated protein kinase/Akt activation beyond its lipid-lowering actions.**
  33. Reymond N, d'Agua BB, Ridley AJ. Crossing the endothelial barrier during metastasis. *Nat Rev Cancer* 2013;13:858-70
  - **Comprehensive summary of the mechanisms involved in cancer cell diapedesis.**
  34. Wang X, Ferreira AM, Shao Q, et al. Beta3 integrins facilitate matrix interactions during transendothelial migration of PC3 prostate tumor cells. *Prostate* 2005;63:65-80
  35. Woodward J. Crossing the endothelium: E-selectin regulates tumor cell migration under flow conditions. *Cell Adh Migr* 2008;2:151-2
  36. Strell C, Niggemann B, Voss MJ, et al. Norepinephrine promotes the beta1-integrin-mediated adhesion of MDA-MB-231 cells to vascular endothelium by the induction of a GROalpha release. *Mol Cancer Res* 2012;10:197-207
  37. Szpak K, Wybierska E, Niedzialkowska E, et al. DU-145 prostate carcinoma cells that selectively transmigrate narrow obstacles express elevated levels of CX43. *Cell Mol Biol Lett* 2011;16:625-37
  38. Guan K, Czyz J, Furst DO, et al. Expression and cellular distribution of alpha(v)integrins in beta(1)integrin-deficient embryonic stem cell-derived cardiac cells. *J Mol Cell Cardiol* 2001;33:521-32
  39. Ryszawy D, Sarna M, Rak M, et al. Functional links between Snail-1 and Cx43 account for the recruitment of Cx43-positive cells into the invasive front of prostate cancer. *Carcinogenesis* 2014;35:1920-30
  40. Wojciak-Stothard B, Potempa S, Eichholtz T, et al. Rho and Rac but not Cdc42 regulate endothelial cell permeability. *J Cell Sci* 2001;114:1343-55
  41. Miekus K, Czernik M, Sroka J, et al. Contact stimulation of prostate cancer cell migration: the role of gap junctional coupling and migration stimulated by heterotypic cell-to-cell contacts in determination of the metastatic phenotype of Dunning rat prostate cancer cells. *Biol Cell* 2005;97:893-903
  42. Daniel-Wojcik A, Misztal K, Bechyne I, et al. Cell motility affects the intensity of gap junctional coupling in prostate carcinoma and melanoma cell populations. *Int J Oncol* 2008;33:309-15
  43. Quadri SK. Cross talk between focal adhesion kinase and cadherins: role in regulating endothelial barrier function. *Microvasc Res* 2012;83:3-11

44. Leesnitzer LM, Parks DJ, Bledsoe RK, et al. Functional consequences of cysteine modification in the ligand binding sites of peroxisome proliferator activated receptors by GW9662. *Biochemistry* 2002;41:6640-50
45. Czyz J, Szpak K, Madeja Z. The role of connexins in prostate cancer promotion and progression. *Nat Rev Urol* 2012;9:274-82
- **In this review, we summarize the data that provide the rationale for implementation of the analyses of connexin function in the studies on metastatic cascade of prostate cancer.**
46. Rushworth GF, Megson IL. Existing and potential therapeutic uses for N-acetylcysteine: the need for conversion to intracellular glutathione for antioxidant benefits. *Pharmacol Ther* 2014;141:150-9
47. van Zijl F, Krupitza G, Mikulits W. Initial steps of metastasis: cell invasion and endothelial transmigration. *Mutat Res* 2011;728:23-34
48. Pollmann MA, Shao Q, Laird DW, et al. Connexin 43 mediated gap junctional communication enhances breast tumor cell diapedesis in culture. *Breast Cancer Res* 2005;7:R522-34
49. Friedl P, Alexander S. Cancer invasion and the microenvironment: plasticity and reciprocity. *Cell* 2011;147:992-1009
- **Summary of the mechanisms that contribute to the generation of diverse cancer invasion routes and programs, potentially crucial for cancer cell diapedesis and metastatic dissemination.**
50. Bravo-Cordero JJ, Hodgson L, Condeelis J. Directed cell invasion and migration during metastasis. *Curr Opin Cell Biol* 2012;24:277-83
51. Garcia-Roman J, Zentella-Dehesa A. Vascular permeability changes involved in tumor metastasis. *Cancer Lett* 2013;335:259-69
52. Doser K, Guserle R, Nitsche V, et al. Comparative steady state study with 2 fenofibrate 250 mg slow release capsules. An example of bioequivalence assessment with a highly variable drug. *Int J Clin Pharmacol Ther* 1996;34:345-8
53. Kajosaari LI, Backman JT, Neuvonen M, et al. Lack of effect of bezafibrate and fenofibrate on the pharmacokinetics and pharmacodynamics of repaglinide. *Br J Clin Pharmacol* 2004;58:390-6
54. Uetake D, Ohno I, Ichida K, et al. Effect of fenofibrate on uric acid metabolism and urate transporter 1. *Intern Med* 2010;49:89-94
55. Hu L, Wu H, Niu F, et al. Design of fenofibrate microemulsion for improved bioavailability. *Int J Pharm* 2011;420:251-5
56. Mroue RM, El Sabban ME, Talhouk RS. Connexins and the gap in context. *Integr Biol (Camb)* 2011;3:255-66
57. Okayasu T, Tomizawa A, Suzuki K, et al. PPARalpha activators upregulate eNOS activity and inhibit cytokine-induced NF-kappaB activation through AMP-activated protein kinase activation. *Life Sci* 2008;82:884-91
- **A study showing the beneficial effects of PPARα activators on endothelial cells attributed to the induction of AMP-activated protein kinase/ Akt activation.**
58. Alexander JS, Zhu Y, Elrod JW, et al. Reciprocal regulation of endothelial substrate adhesion and barrier function. *Microcirculation* 2001;8:389-401
59. Deguchi S, Sato M. Biomechanical properties of actin stress fibers of non-motile cells. *Biorheology* 2009;46:93-105
60. Yuan SY, Shen Q, Rigor RR, et al. Neutrophil transmigration, focal adhesion kinase and endothelial barrier function. *Microvasc Res* 2012;83:82-8
61. Friedl P, Wolf K. Plasticity of cell migration: a multiscale tuning model. *J Exp Med* 2010;207:11-19
62. Nevo I, Sagi-Assif O, Meshel T, et al. The involvement of the fractalkine receptor in the transmigration of neuroblastoma cells through bone-marrow endothelial cells. *Cancer Lett* 2009;273:127-39

### Affiliation

Katarzyna Piwowarczyk<sup>1</sup>, Ewa Wybieralska<sup>1</sup>, Jarosław Baran<sup>2</sup>, Julia Borowczyk<sup>3</sup>, Paulina Rybak<sup>4</sup>, Milena Kosińska<sup>1</sup>, Anna Julia Włodarczyk<sup>5</sup>, Marta Michalik<sup>1</sup>, Maciej Siedlar<sup>2</sup>, Zbigniew Madeja<sup>1</sup>, Jerzy Dobrucki<sup>4</sup>, Krzysztof Reiss<sup>6</sup> & Jarosław Czyż<sup>1</sup>

<sup>†</sup>Author for correspondence

<sup>1</sup>Jagiellonian University, Department of Cell Biology, Faculty of Biochemistry, Biophysics and Biotechnology, Krakow, Poland

E-mail: jarek.czyz@uj.edu.pl

<sup>2</sup>Polish-American Institute of Pediatrics, Jagiellonian University Medical College, Department of Clinical Immunology, Krakow, Poland

<sup>3</sup>Jagiellonian University, Department of Cell Biology, Faculty of Biochemistry, Biophysics and Biotechnology, Laboratory of Tissue Engineering, Krakow, Poland

<sup>4</sup>Jagiellonian University, Division of Cell Biophysics, Faculty of Biochemistry, Biophysics and Biotechnology, Krakow, Poland

<sup>5</sup>Cardiff University, School of Biosciences, Cardiff, UK

<sup>6</sup>School of Medicine, Stanley S. Scott Cancer Center, LSU Health Sciences Center, Neurological Cancer Research, New Orleans, USA

### Supplementary materials are available online.

Figures S1 and S2.